UDC 621.224.7+621.313.32

SITE TEST OF 500M 206MW PUMP-TURBINE AND 220MVA GENERATOR-MOTOR

Tsuneo Ueda
Yoshiyuki Niikura
Kazumasa Ajiro
Shoji Sato
Akira Oshitani

I. FOREWORD

Since the pump-turbines and generator-motors for Chongpyong Power Station, Korea Electric Company, are the epock-making high-head large-capacity machines, the most advanced technology was employed and the studies were conducted from every angle to make perfection more perfect at the design stage. As the result, the installation and the test were completed in such a short period of time-about 11 months after starting the erection of pump-turbine spiral casing. And the unit No. 1 entered the commercial operation from November 1, 1979, and the unit No. 2 from February 1, 1980.

In the test at site, a large amount of test data was collected and analyzed by fully exercising the most advanced data collecting and analyzing technology. Also, these test data were compared with the model test data and the design data, thus providing the precious data to the design and manufacture of a future large-capacity pump-turbine and generator-motor.

We herein introduce a part of the site test data for reference of engineers concerned.

II. GENERAL DESCRIPTION OF PUMP-TURBINES AND GENERATOR-MOTORS

Congpyong Pumped-storage Power Plant is a pure pumped-storage power station using the upper reservoir of the existing Chongpyong Power Station as its lower reservoir. As shown in *Fig. 1*, the water from the upper reservoir is led to two 206MW pump-turbines through two penstocks about 800m long and is discharged to the lower reservoir by way of two surge tanks in the tailrace and one trailrace

Table 1 Main data of pump-turbine and generator-motor

(a) Pump-turbine

Q'ty	2
Type	Vertical shaft, reversible Francis pump-turbine
Specifications of turbine	
Maximum output	206,000kW
Effective head	473/452/437.5m (max/rated/min)
Turbine discharge	52.49m³/s
Speed	450 rpm
Specific speed	98.0 (m·kW)
Specifications of pump	
Total dynamic head	498.5/474m (max/min)
Pumps discharge	39m³/s
Maximum input	206,100kW
Speed	450 rpm
Specific speed	27.7 (m·m³/s)

(b) Generator-motor

Q'ty	2	
Type	Vertical shaft, totally enclosed separately fan-ventilated air cooled, three-phase AC synchronous generator-motor; air cooler and separate motor-driven fan provided.	
Rating	Generator	Motor
Output	220,000kVA	220,000kW
Voltage	13.8kV	13.8kV
Frequency	60Hz	60Hz
Speed	450 rpm	450 rpm
Power factor	0.91 (lag)	1.0
Bearing arrangement	Conventional type (IM8421, IEC), magnetic thrust bearing provided	

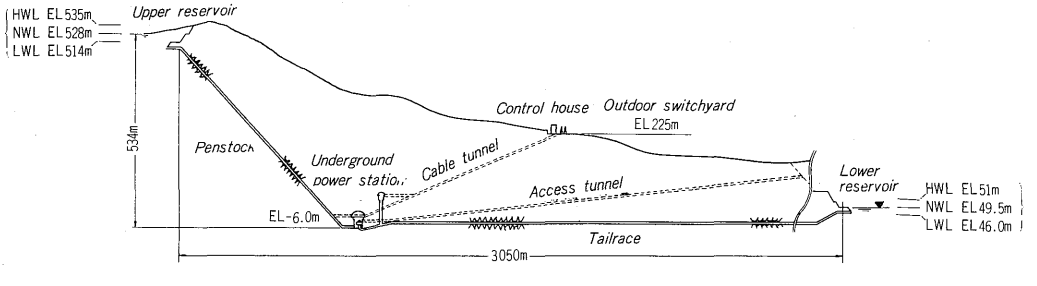

Fig. 1 Cross section of waterway

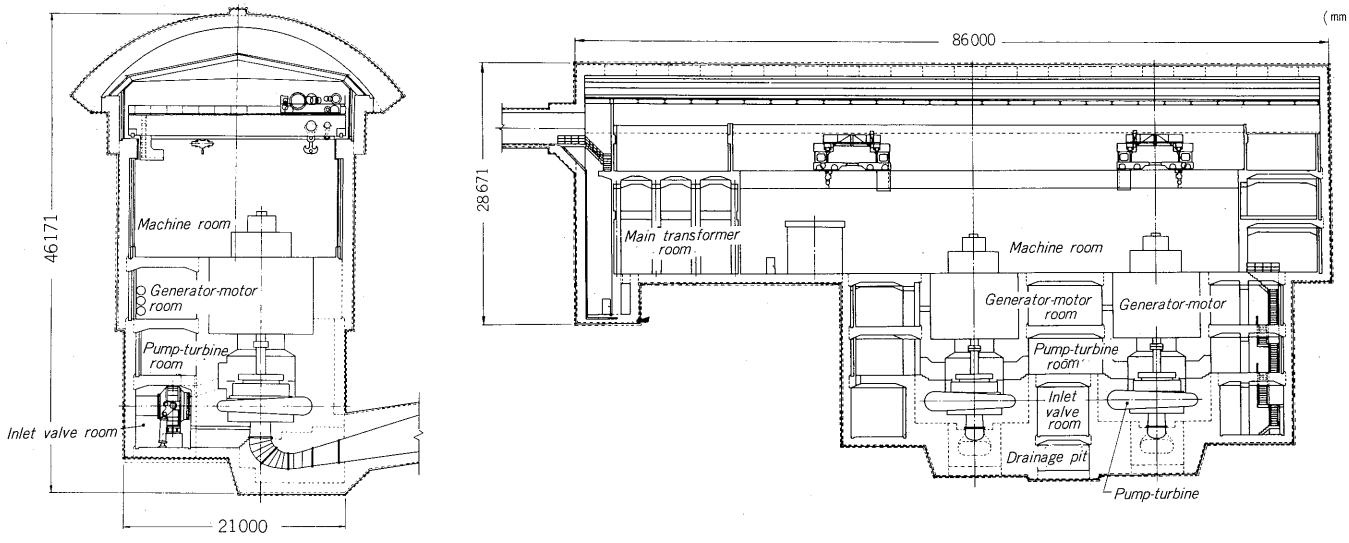

Fig. 2 Cross section of power house

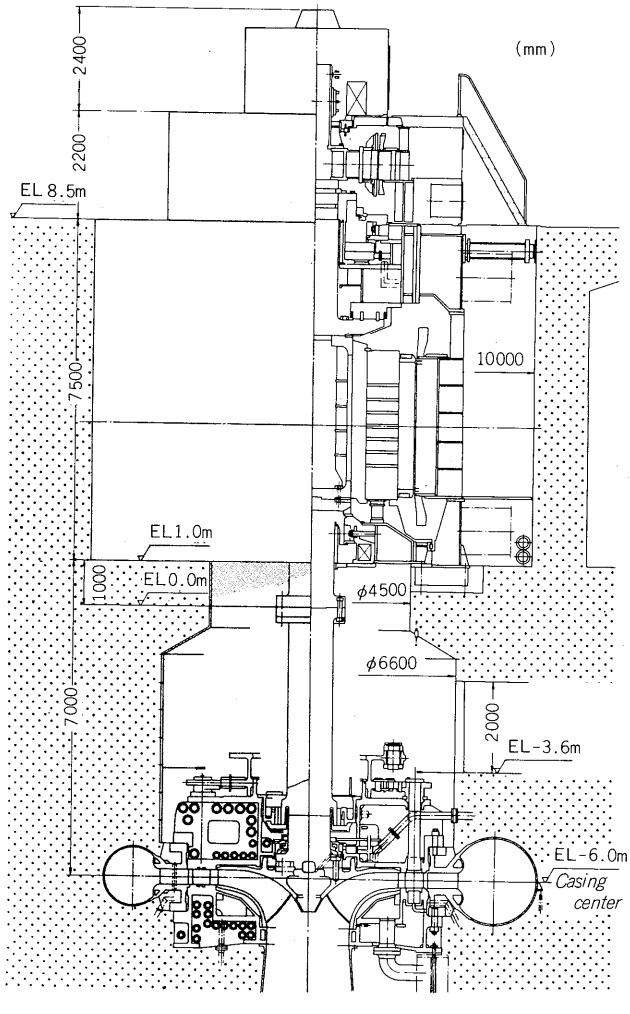

Fig. 3 Cross section of pump-turbine and generator-motor

about 2,000m long.

The cross section of power house is shown in *Fig. 2*, the specifications of pump-turbines and generator-motors in *Table 1*, and the cross section of pump-turbines and generator-motors in *Fig. 3*.

The pump-turbines and generator-motors have the following features.

1. Pump-turbine

1) The performance has been improved by the use of computer program for runner design and flow analysis. Especially, a great improvement has been achieved in the efficiency at a partial load of turbine.

2) Every kind of characteristic data, including hydraulic thrust in the axial direction and runner load in the radial direction, was measured using a model of pump-turbine with water passage completely homologous with those of prototype.

3) The detailed analysis was conducted on stress and strain by the finite element method, and thus the rational structure was developed. Specifically speaking,

(1) The parallel type stay ring peculiar to us, which has an excellent performance and strength, was adopted.

(2) In order to reduce the load imposed on the foundation, the balance type discharge ring was employed.

4) The balance type main shaft seal peculiar to us was adopted.

5) The runner and wicket gate materials were of high-nickel 13-chromium stainless cast steel, which shows an excellent strength and weldability.

2. Generator-motor

1) By using the magnetic thrust bearing peculiar to us, the frictional resistance of thrust bearing in pumping start has been reduced, the reliability of thrust bearing operating at a high speed and carrying a heavy load has been improved,

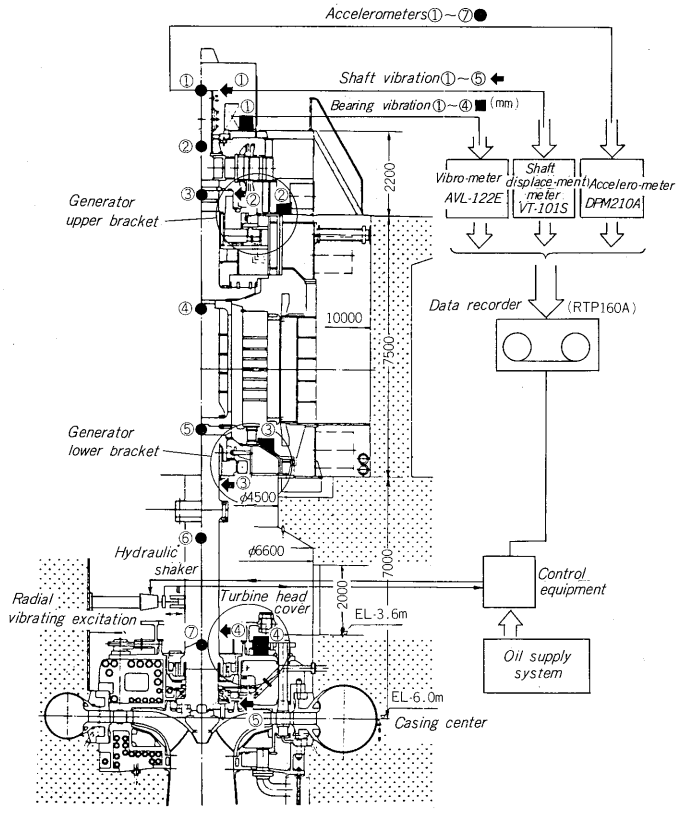

Fig. 4 Measuring system of shaft vibration

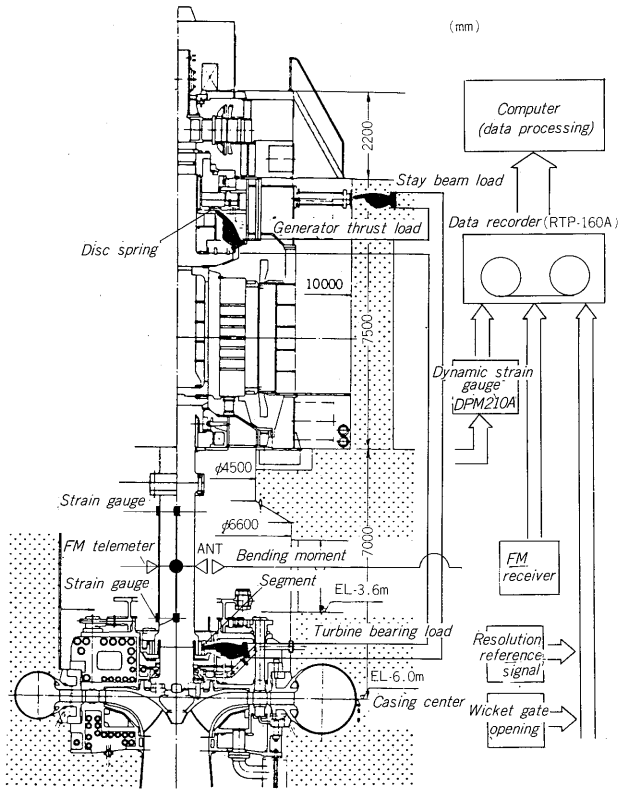

Fig. 5 Measuring system of radial force and axial thrust of runner

and the loss of thrust bearing during operation has been reduced.

2) In order to reduce vibration, the stiffness of guide bearing structure was improved, and the stiffness was checked to be sure by the finite element method. Specifically speaking,

(1) The cotter type was adopted as the segment supporting method of guide bearing instead of screw type.

(2) In order to increase the supporting stiffness of upper guide bearing, the stay beam was employed.

3) The detail vibration analysis of bearing stated below was carried out.

(1) In calculating natural frequency, the elasticity and damping of oil film, magnetic pullforce and gyro-moment were taken into account. Also, to calculate the vibration at the points in the shaft system in various kinds of operation modes, the random response analysis and the direct response analysis were executed.

III. SITE TEST DATA COLLECTING SYSTEM AND ANALYZING SYSTEM

In addition to the measurement of vibration, pressure, stress, and deformation, the following special tests were carried out.

1. Measurement of vibration response of main shaft system

In case of a high-head pump-turbine and generator-motor, it is especially important to obtain the accurate data on the vibration response of main shaft system at the design stage. In this connection, in order to improve the future calculative accuracy, the vibration response of main shaft system was measured when the installation at site was completed. *Fig. 4* shows the measuring system of shaft vibration.

1) The constant exciting force of sine wave was given to the shaft system in radial and axial directions by the 8 ton hydraulic dynamic shaker, and the vibration response was measured by detecting vibrations induced at measuring points. In taking measurement, the initial force was maintained constant, and the frequency of exciting force was varied from 0.5Hz to 50Hz at a apeed of about 0.1Hz/sec.

2) The hydraulic dynamic shaker consists of a actuator operated by an electric signal of sine wave from the controller and a piston operated by a signal from the actuator.

The exciting force of sine wave generated at the piston is transmitted to the shaft system to be tested through the load cell mounted at the top of piston and the roller. The exciting force detected by the load cell is fed back to the controller to maintain the exciting force constant. The exciting force was set at 1,000kg ±500kg.

3) The vibration of shaft and runner was measured by an eddy current type proximitors, and the vibration excited on guide bearings with a vibrometer and an accelerometer.

4) The excited vibrations and exciting force were recorded by a 28-channel data recorder in real time. In order to perform the high-speed simultaneous process of the data of

malti-channels, a computer in the exclusive use for analysis by means of real time spectrum analyzer was used.

2. Measurement of dynamic hydraulic load for runner

In order to estimate the vibration of shaft in various kinds of operation modes, the radial hydraulic load, hydraulic moment, and axial hydraulic thrust acting on the runner were measured because they are major causes of vibration. The measuring system is shown in *Fig. 5*.

1) To measure the radial load of runner, it is necessary to measure the load reactions on the pump-turbine guide bearing and the bending moment acting in two sectional planes of the pump-turbine shaft.

2) To obtain the load reactions of pump-turbine guide bearing, strain gauges were stuck on guide bearing segment pads, and the respective load reactions of guide bearing were measured. As for the measurement of the bending moment produced on the turbine shaft, strain gauges were stuck on the shaft in two directions being at right angles to each other, and the change in electrical resistance caused by strain was picked up from the shaft with the FM telemeter and was recorded by the data recorder after demodulation.

3) As for the measurement of the axial hydraulic thrust acting on the runner, strain gauges were stuck on the disc spring supporting the thrust bearing segment pads of generator-motor to measure strain and thus to obtain the load reactions of thrust bearing.

3. Measurement of runner vane stress

The static stress induced in the runner vane by static pressure and centrifugal force can be calculated by the three-dimensional finite element method using the pressure distribution calculated by the use of the flow analyzing computer program. However, to obtain the dynamic stress caused by unsteady flow during the transient condition, it is needed to make an actual measurement.

To measure the stress of runner vane, water-proof strain gauges were stuck on the runner vane, and the change in electric resistance due to strain was taken outside by means of the FM telemeter mounted on the runner cone and the antenna mounted on the wall of upper draft tube and then was recorded by the data recorder after demodulation.

4. Hydraulic torque of wicket gate

Strain gauges were stuck on the wicket gate shaft to measure the hydraulic torque of wicket gate.

IV. RESULTS OF MEASUREMENT AND STUDY OF THEM

1. Natural frequency of main shaft system

The following two kinds of exciting tests were conducted.

1) Exciting test at standstill

Main shaft was excited with a bearing clearance being zero by the 8 ton hydraulic dynamic shaker while the unit was at a standstill.

2) Exciting test at running

Main shaft was excited with an ordinary clearance of bearing while the main machines were running. The measured values pertaining to the natural frequency of main shaft were compared with calculated values in *Table 2* and *Fig. 6*. This comparison reveals that measured and designed values agree well with each other, and thus it has been confirmed that there exists an ample allowance concerning runaway speed.

The calculation was carried out by the use of the natural frequency calculating computer program, which takes into account the elasticity of bearing, gyro-moment, and magnetic pulforce of generator.

In order to improve the accuracy of calculating the natural frequency of shaft, the following items should be clarified.

(1) Stiffness of bearing supporting structure
(2) Elasticity of bearing oil film
(3) Additional mass of water to runner

The actual stiffness of bearing supporting structure was

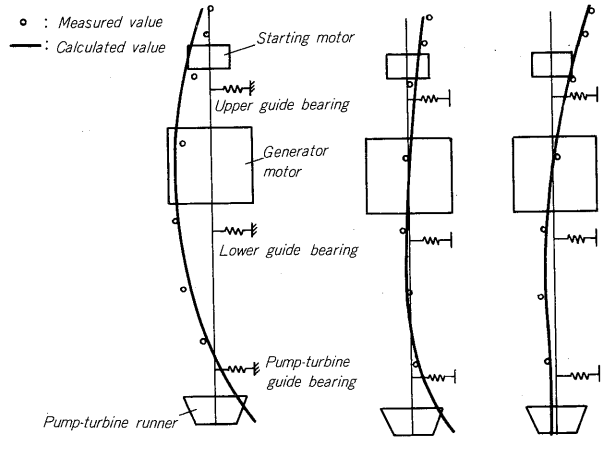

Fig. 6 Mode of natural frequency of shaft

Table 2 Natural frequency of shaft

	Natural frequency (Hz)					
	First order		Second order		Third order	
	Measured	Calculated	Measured	Calculated	Measured	Calculated
0 rpm, in water, bearing clearance: 0 mm	13.1	14.1	14.7	15.9	19.6	20.3
450 rpm, in no water, bearing clearance: design value	11.6	12.4	15.5	16.2	17.9	18.1
450 rpm, in water, bearing clearance: design value	11.4	12.2	13.1	14.2	17.7	17.9

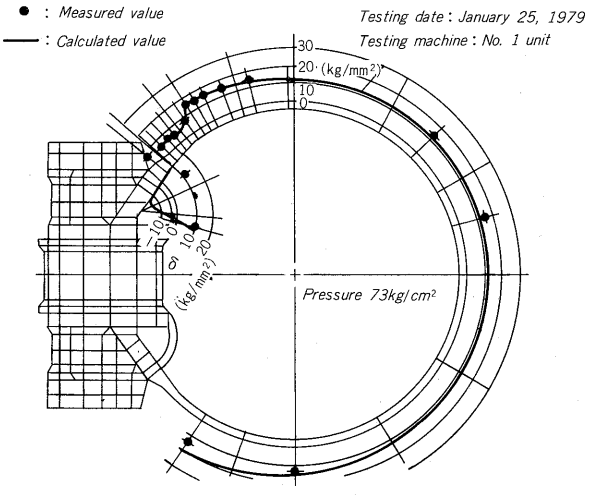

Fig. 7 Stress distribution of spiral casing

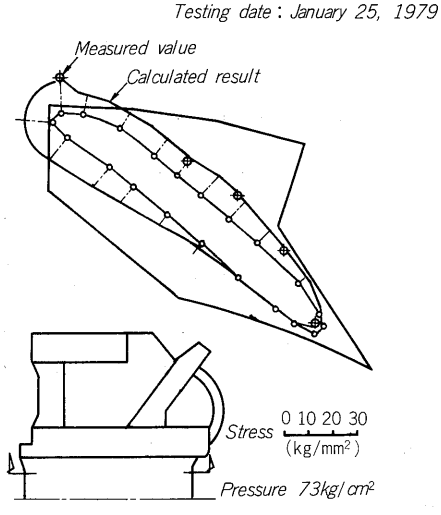

Fig. 8 Stress distribution of stay vane

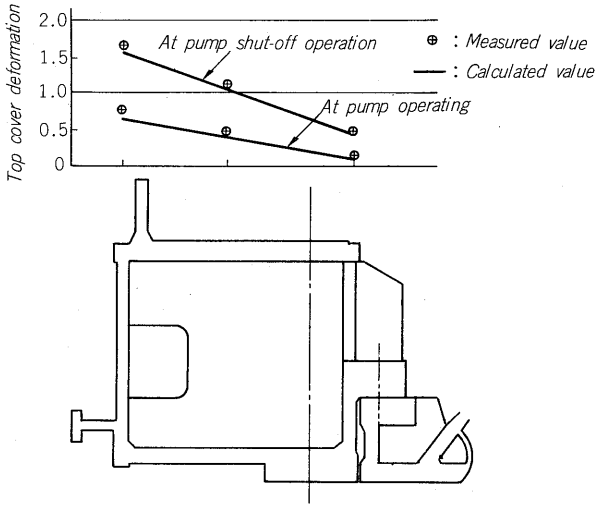

Fig. 9 Deformation of head cover

estimated by comparing the following two:

(1) Natural frequency calculated using the supporting stiffness of bearing obtained by the finite element method.

(2) Measured value by the exciting test at standstill without oil film.

The comparison between natural frequencies at a standstill and running states revealed that the elasticity of oil film was about 5×10^5 kg/mm at a rated speed.

As for the effect of additional mass of water to the runner, the comparison between natural frequencies with and without water while running the machines revealed the following:

(1) The additional mass of water to the runner has almost no effect on the first and third order natural frequencies; however, it reduces the second natural frequency by about 15%. As known from *Fig. 6*, (b), this is because the runner determines the mode of the secondary natural frequency.

(2) The additional mass of water to the runner is 0.8 to 1.0 time of the runner weight.

2. Measurement of stress and strain

1) Stress of spiral casing and stay vane

Fig. 7 and *Fig. 8* show the stress induced respectively in the spiral casing and the stay vane at a hydraulic pressure test of spiral casing (test pressure: 73kg/cm^2) and makes a comparison between stresses measured and calculated by the finite element method. These figures indicate that the two agree well with each other.

2) Deformation of head cover

Fig. 9 shows the measured vertical displacements of head cover at pump shut-off and pumping operation and their corresponding ones calculated by the finite element method. This comparison indicates that they agree well with each other.

3. Metal running

Since the upper reservoir has no water source, this power plant is a pure pumped storage power plant. For this reason, the metal running was carried out with the draft tube water level being blown down and the machine being revolved in the pumping direction by the starting motor.

Fig. 10 shows the temperature characteristics of guide bearings and sealing parts at the metal running in the pumping direction.

Since a temperature rise is low even at the sealing parts of runner, it has been confirmed that a long time spinning reserve in pumping is possible.

4. Initial pumping test

The initial pumping test, which is technically the most difficult of the site tests of pump-turbine, was conducted in the following procedures.

1) First, the tailrace gate was opened to fill the tailrace tunnel with water. Then, the penstock drain valve and the spiral casing drain valve were opened to fill the penstock with water as high as the water level of the lower reservoir.

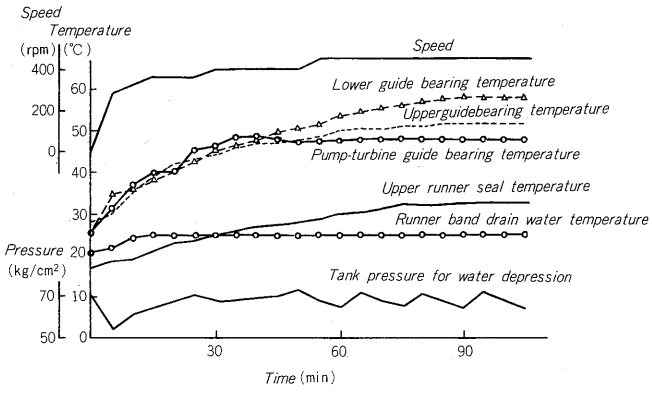

Fig. 10 Metal running at pump direction

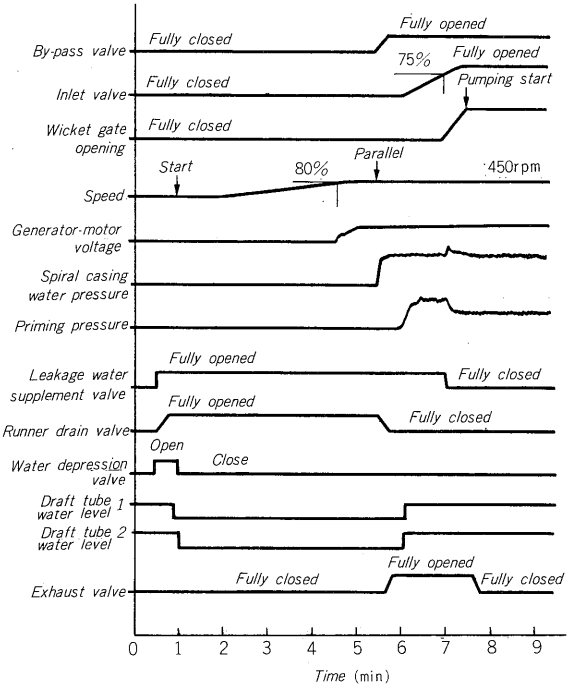

Fig. 11 Pump start sequence

2) Since the upper reservoir of this power plant has no water source, the water was taken from the tailrace with the inlet valve and wicket gate fully closed and it took about 3 days to fill the penstock with water to as high a level as the intake by the temporarily installed pump and piping.

3) Although a static head of 454m achieved by this filling was lower than the guaranteed minimum head of 474m, the initial pumping was carried out with the opening of wicket gate being reduced to the best opening of 75%.

The test results were quite satisfactory without any vibration and other abnormalities.

5. Characteristics of pumping start operation

The sequence of pumping start is shown in *Fig. 11*.

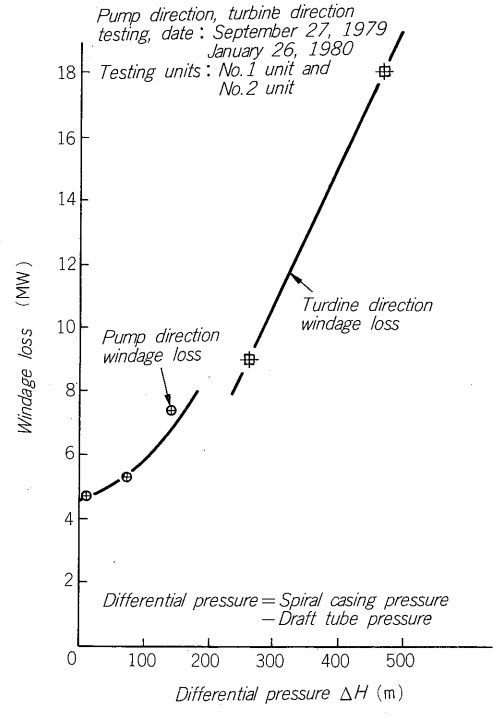

Fig. 12 Windage loss of pump-turbine

1) Depression of water level and start

The pumping operation was started by the 19.5MW starting motor coupled with generator-motor on its top. In order to reduce the capacity of starting motor and shorten the accelerating time, the water level of runner chamber was depressed by the pressure air, and the runner was started in the air. When the speed reached the rating, it was paralleled with the electric system.

It was confirmed that the pump-turbine windage loss at the rated speed, as shown in *Fig. 12*, had sufficiently an allowance against the starting motor capacity and also was exerted a less influence on by the spiral casing water pressure, because of the less leakage effected by wicket gate seal and of the excellent drainage performance through the runner band drainage hole.

2) Air exhaust, establishment of priming pressure

After completing the synchronization with the electric system, the air is exhausted by opening the air exhaust valve. If the exhaust of air is insufficient, the priming pressure is not established and thus pumping cannot be started. In case of this plant, since the optimum location of exhaust hole had been selected by a model test, the priming pressure was built up smoothly.

3) Completion of air exhaust, start of pumping

Even after the priming pressure has been established, exhausting is continued for another 1 minute to completely exhaust the residual air from the runner chamber. Then, the wicket gate is opened to the best opening to enter the normal pumping operation.

As shown in *Fig. 13*, vibration on the way of opening the wicket gate is small, and thus the normal pumping operation was smoothly accomplished.

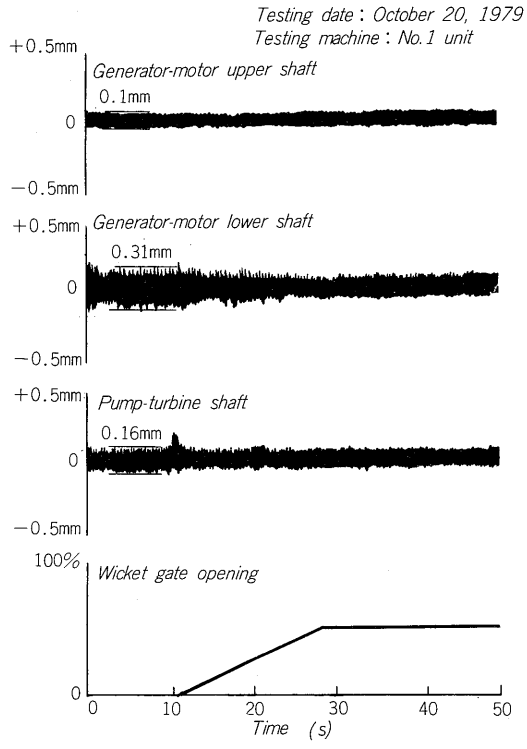

Fig. 13 Shaft vibration at pumping start

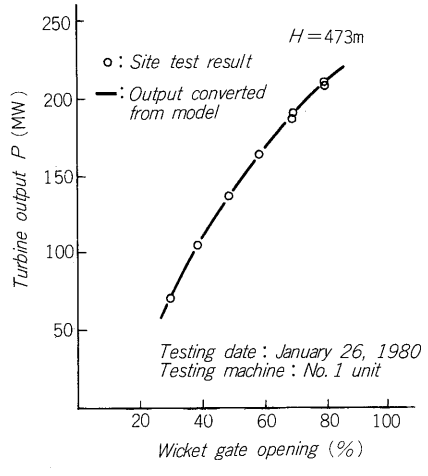

Fig. 14 Output test of pump-turbine

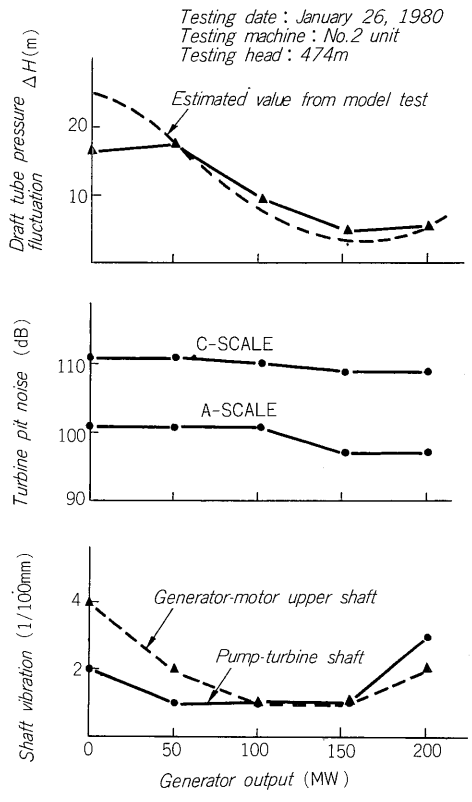

Fig. 15 Vibration and noise characteristics at turbine operation

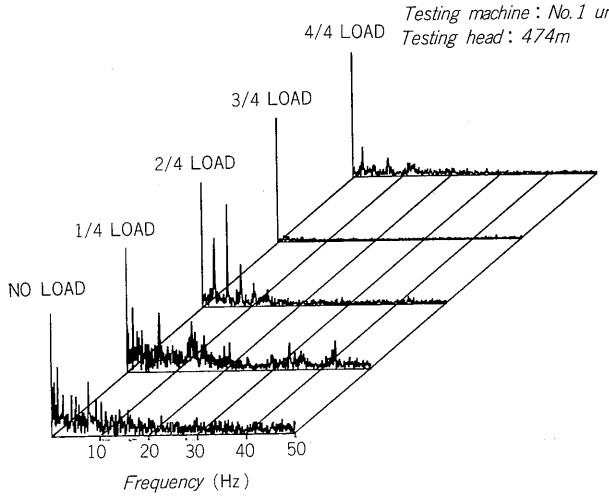

Fig. 16 Frequency spectrum analysis of draft tube pressure fluctuation at turbine operation

6. Turbine operating performance

Fig. 14 shows the results of turbine output test. The test results agree well over all the range of operation with the converted characteristic of the model test results.

Fig. 15 shows the relations of output to vibration, noise, and pressure fluctuation.

It was confirmed that the turbine could be operated over all the output range without supplying the air to the draft tube, because the absolute value of vibration was small, although the vibration and noise increased slightly at an output of below 100MW.

The draft tube pressure fluctuation derived from the model test results agrees well with the measured value.

According to the frequency spectrum of draft tube pressure fluctuation shown in *Fig. 16*, the pressure fluctuations due to the slight surging are observed at 1/3 and 2/3 of the rotating cycle at 50% load. This is caused by two vortex ropes at the upper draft tube and agrees well with the observations of model test results.

7. Pump input rejection, and turbine load rejection

Fig. 17 show the transient phenomena at a pump input rejection test of 204MW, and *Fig. 18* that a maximum turbine output rejection test of 206MW.

Both cases well agree with the transient phenomena calculated by a computer on the basis of the four quardrant characteristics obtained by a model test.

8. Hydraulic axial thrust

In order to make the lifting force of the magnetic thrust bearing as large as possible and thus to reduce the loss of the mechanical thrust bearing during normal operation, it is necessary to estimate the hydraulic axial thrust in every kind of operation mode including transient phenomena.

To achieve these ends, the hydraulic axial thrust was measured in a model test with the shape of water chamber between the runner and the head cover/discharge ring, balance pipe, etc. being made homologous to the prototype. And it has been confirmed that the measured hydraulic axial thrust in the site test agrees well with the converted hydraulic axial thrust of the model test results.

Fig. 19 shows the measured hydraulic axial thrusta. In *Fig. 19*, the lift-up load by the magnetic thrust bearing is also indicated. It is known from *Fig. 19* that the load of the mechanical thrust bearing during the normal operation is greatly reduced.

The reduction in the frictional loss of the mechanical thrust bearing at turbine full load is 340kW. The exciting current of the magnetic thrust bearing required to achieve this reduction is 140A at 23V, that is, the required exciting power is only 3.2kW. Consequently, the efficiency of generator-motor at full load improves by 0.15%.

9. Radial hydraulic runner load

In order to make the vibration analysis of the shaft system at the design stage, a radial hydraulic force acting on the runner was measured at a model test. And it was confirmed that the measured radial hydraulic runner load in the site test agreed well the converted value from the model test results.

Fig. 20 shows the radial runner load fluctuation in the event of a load rejection.

As for the fluctuation in radial hydraulic runner load, the maximum appears in the zone of braking torque at the

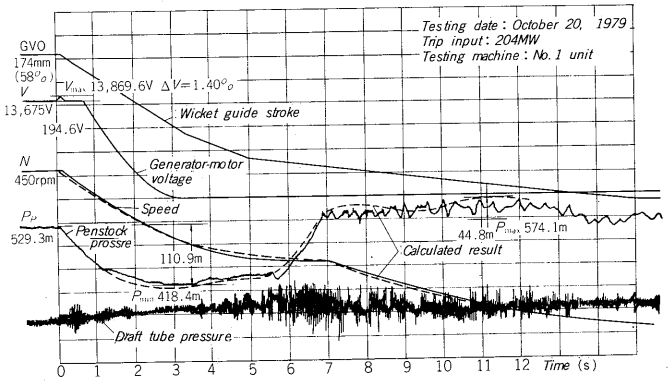

Fig. 17 Test results of pump trip

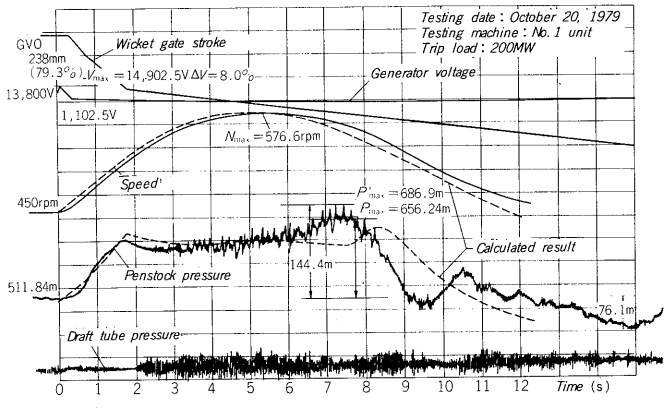

Fig. 18 Test results of full load rejection

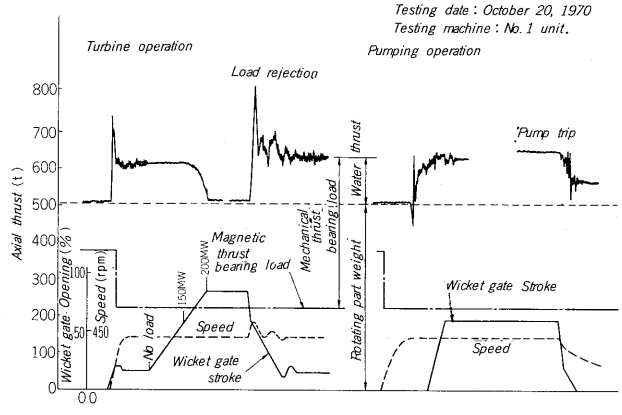

Fig. 19 Hydraulic axial thrust

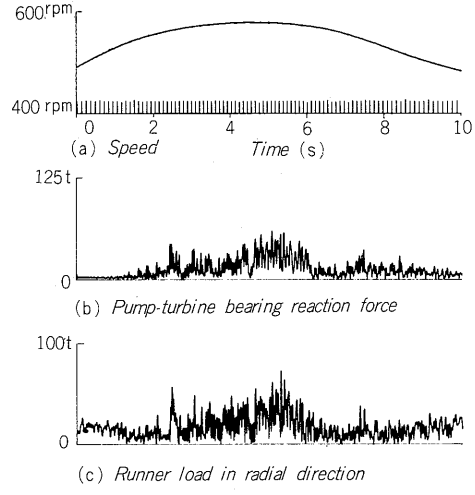

Fig. 20 Radial hydraulic force acting on runner at turbine load rejection

third quardrant, and the peak frequency is about 2/3 of the rotating cycle. In this case, the peak frequency of the draft tube pressure fluctuation is about 1/2 of the rotating cycle.

Fig. 21 indicates the fluctuation in radial hydraulic runner load in the event of an input rejection. Immediately after the water flow has been reversed from the pumping direction to the turbine direction, the fluctuation in radial hydraulic runner load reaches its maximum, and the peak frequency is about 90% of the rotating cycle. In this case, the peak frequency of the draft tube pressure fluctuation is about 2/3 of the rotating cycle.

As know from *Figs, 20* and *21*, the fluctuation in radial hydraulic runner load during the normal operation is far smaller as compared with the transient one.

10. Vibration of runner

Since the fluctuation in radial hydraulic runner load becomes big, the vibration of the overhung runner becomes large in the transient operation. In this connection, since a high-head pump-turbine requires the runner seal clearance to be made small so as to reduce the leakage loss at the runner sealing section, there is a fear of a possible rubbing between the runner and the stationary part.

To check for this conceivable rubbing, an eddy-current type proximitor was mounted on the runner sealing section in the site test to measure the vibration of event of a turbine full load rejection, and *Fig. 23* the one in the event of a pump input rejection (locus of the runner center).

The maximum amplitude of runner vibration is about 1.9mm, in other words, 60% of the runner seal clearance. That is, it was confirmed that there was no possibility of the rubbing between the runner and the stationary part.

The calculated runner vibration obtained by F.E.M., which has inputted a radial hydraulic runner load and moment described in the previous section has proved to agree well with the measured runner vibration.

This shows explicitly that the further improvement in the measuring accuracy of radial runner load in a model test will make it possible to estimate a vibration of runner and shaft in every kind of operation mode at the design stage.

11. Runner vane stress

The stress analysis by the finite element method revealed that the maximum stress appeared at the root of

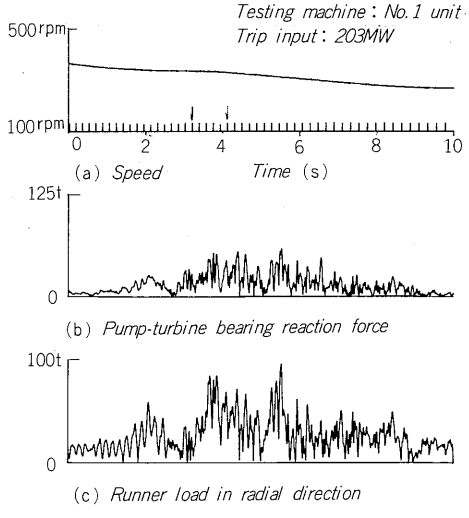

Fig. 21 Radial hydraulic force acting on runner at pump input rejection

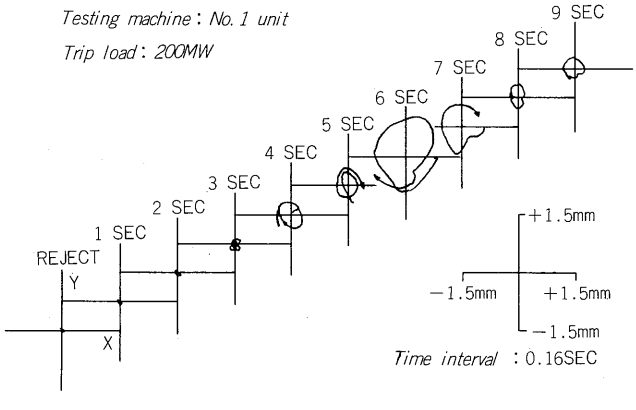

Fig. 22 Runner vibration at turbine load rejection

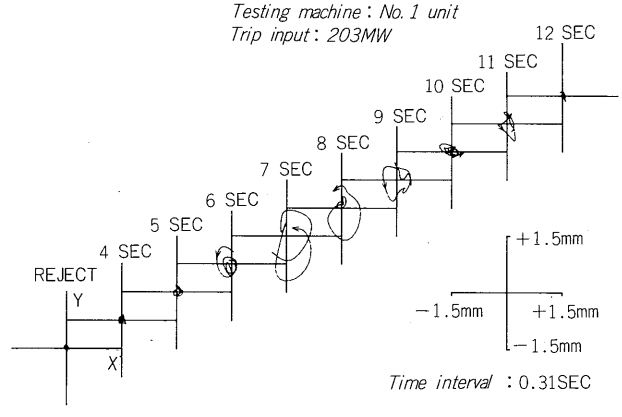

Fig. 23 Runner vibration at pump input rejection

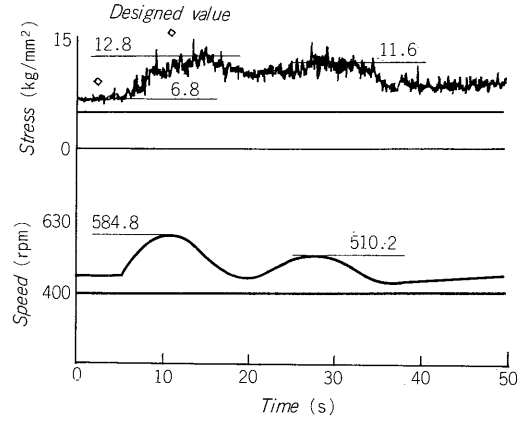

Fig. 24 Runner vane stress at turbine load rejection

Table 3 Summary of field test data for unit No. 2

[Normal operation]

Test date: 23, Jan. 1980

			Generating (200 MW) operation	Pumping operation	Remarks
Upper reservoir (m)			533.06	534.75	
Lower reservoir (m)			50.59	50.50	
Vibration (μm) peak to peak	*1 V1	Generator-motor upper bracket (H)	7.0	6	Allowable value (by VDI 2056) 200 μ
	V2	Generator-motor lower bracket (H)	5.5	5.5	200 μ
	V3	Pump-turbine head cover (H)	7.0	12	200 μ
					*1 Measured point (Refer to attached drawing.)
Shaft run-out (μm)*2 peak to peak	R1	Generator-motor upper shaft (40)	20	10	Target data (Specification) 200 μm
	R2	Generator-motor lower shaft (120)	20	30	200 μm
	R3	Pump-turbine shaft (80)	30	15	200 μm
		( ) is static run-out.			*2 Corrected value with static run-out
Generator-motor stator winding temperature rise (°C)			53	51	Guaranteed value not more than 80°C (Measured on Jan. 26, 1980)
Bearing temperature (°C)		Generator-motor upper bearing	51	51	Guaranteed value
		Generator-motor lower bearing	51	50	Not more than 65°C
		Generator-motor thrust bearing	37	43	
		Pump-turbine bearing	47.5	45.5	(Cooling water 25°C)
			(Cooling water 3 °C)		

[Transient operation]

	200 MW load rejection	Pump input rejection	Remarks
Max. speed rise (%)	28.5	–	Guaranteed value not more than 40%
Max. pressure rise (m)	683.0	568.28	Not more than 730m (The value includes high frequency fluctuation.)
Max. voltage rise (%)	9.09	–	Not more than 20%

runner vane inlet on the side of runner crown in the event of a turbine full load rejection. This stress was measured and the results are shown in *Fig. 24*. It was confirmed that the measured stress well agreed with the calculated one and was below the allowable stress.

V. SUMMARY AND ACKNOWLEDGEMENT

As a result of the carefull studies and work at the design manufacture, and installation stages, the high-head pump-turbine and generator-motor for the Chongpyong Pumped-storage Power Plant was not caught in trouble at the stage of test run and entered the commercial operation 2 months earlier than scheduled. At present, these units are operating smoothly. *Table 3* gives the overall performance of No. 2 unit.

We are sure that the precious data collected in the site test contributes greatly to the development of the equipments for a future high-head large-capacity pumped storage power plant.

To conclude this paper, we acknowledge our indebtedness to persons concerned of Korea Electric Company and Nippon Koei Co., Ltd. for their helpful advice and cooperations in carrying out the installation and test of the pump-turbine and generator-motor.

Bibliography

(1) H. Grein et al.: "Radial Force on Hydraulic Turbomachine" *Zulzer Technical Review*, Jan., 1975